

Interplay between magnetic properties and thermoelectricity in misfit and Na cobaltates

J. Bobroff,¹ S. Hébert,² G. Lang,¹ P. Mendels,¹ D. Pelloquin,² and A. Maignan²

¹Laboratoire de Physique des Solides, Univ. Paris-Sud, UMR8502, CNRS, F-91405 Orsay Cedex, France

²Laboratoire CRISMAT, UMR 6508, CNRS et EnsiCaen, 14050 Caen, France

(Received 27 August 2007; published 28 September 2007)

We present a comparative study of CoO₂ layers in the Bi misfit and Na_xCoO₂ cobaltates. Co NMR measures the *intrinsic* susceptibility of the Co layers and is not affected by spurious contributions. At low dopings where room-temperature thermoelectric power (TEP) is large, Curie-Weiss susceptibilities are observed in both materials. But NMR and muon-spin resonance experiments find neither charge nor spin order down to low temperatures in Bi misfit cobaltates in contrast to the case of Na_xCoO₂. This demonstrates that metallicity, charge, and magnetic order are specific to the Na layers in Na_xCoO₂ whereas strong correlations are generic for cobaltate physics and could explain the large TEP.

DOI: [10.1103/PhysRevB.76.100407](https://doi.org/10.1103/PhysRevB.76.100407)

PACS number(s): 76.60.-k, 71.10.Hf, 74.25.Fy, 76.75.+i

High efficiency of thermoelectric devices is needed to open the way to large-scale applications such as thermoelectric refrigerators or power sources. This relies upon a large figure of merit $ZT=S^2T/\rho\kappa$, where S , the Seebeck coefficient, measures the thermoelectric power (TEP), ρ is the resistivity, κ is the thermal conductivity, and T is the temperature. Combining a large S together with a low resistivity is usually impossible to achieve in standard metals or semiconductors.¹ Many alternatives have been investigated to circumvent this limitation, from rattling skutterudite semiconductors to narrowband heavy fermions. The recent discovery of unexpectedly large ZT in the cobaltates Na_xCoO₂ has opened a new route.² There, orbital or spin degrees of freedom together with strong correlations might be used as an independent source of entropy, resulting in large TEP together with good conductivity.²⁻⁴ However, the origin of this large TEP is still highly debated and not necessarily linked to correlations. It could be caused by specific spin or charge order known to occur in the Co layers,^{5,6} or accounted for by a more conventional metallic picture.⁷ Understanding the origin of the correlations in this promising compound and their interplay with transport and thermoelectric properties is a key element to settle this issue. This would help to decide whether low-dimensional strongly correlated oxides could play a role in the future development of thermoelectricity.

In this frame, we focus on the Bi misfit cobaltates, which display large TEP as well.^{8,9} Bi misfits and Na_xCoO₂ feature identical CoO₂ layers but differ in their dopant layer. In Na_xCoO₂, it consists of a single Na layer where the Na can order structurally. In Bi misfits, it is composed of a thick rocksalt (RS) layer incommensurate with the Co layers,⁸ and the doping is varied by changing its cationic and oxygen composition. This results in a smoother spatial variation of the Coulomb potential due to the dopant layer than in Na_xCoO₂, because of the RS structure, incommensurability, and thickness. By comparing the properties of Bi and Na cobaltates, we are able to distinguish the intrinsic properties of the Co layers from those due to the dopant layer nature. The intrinsic spin susceptibility measured by NMR shows a flat metalliclike behavior at high doping (low x) and a Curie-Weiss behavior at low doping ($x \geq 0.65$), revealing the presence of correlations as in Na_xCoO₂. However, using NMR

and muon-spin resonance (μ SR), we do not find any charge or magnetic order down to low temperatures. Furthermore, Bi misfit cobaltates are found to be much less conducting than Na cobaltates. This comparison demonstrates that large TEP in these oxides is due to strong correlations.

We prepared powder samples of the four-layer Bi family $[\text{Bi}_2M_2O_4]^{\text{RS}} \cdot [\text{CoO}_2]_m$ ($M=\text{Ba, Sr, Ca}$ and m is the misfit ratio), named hereafter BiMCoO, using the procedure detailed in Ref. 8. By changing both the cation M and the oxygen content through thermal treatments, we are able to span the phase diagram in an unprecedentedly large range of doping, equivalent to the domain $x \approx 0.6 \rightarrow 0.9$ in Na_xCoO₂. To access higher TEP and lower dopings than previous studies, BiCaCoO powders were also synthesized in a sealed ampoule with primary vacuum, leading to $S(T=300\text{ K}) = 210 \mu\text{V/K}$, to be compared to the air value $S = 150 \mu\text{V/K}$. Annealing this sample at $T=400^\circ\text{C}$ in oxygen pressure ($P_{\text{O}_2}=100\text{ bar}$) leads to an intermediate value $S = 190 \mu\text{V/K}$. This variation is likely due to a change of the oxygen content, and hence a variation of the CoO₂ layer doping.¹⁰ All structures were checked using x-ray and electron diffraction coupled to energy-dispersive spectroscopy analyses. A four-probe technique and a steady-state method were respectively used to measure resistivity and TEP in a physical properties measurement system, using ceramic bars with ultrasonically deposited indium contacts. The μ SR measurements were performed at PSI (Switzerland). The NMR measurements were carried out in a variable field magnet at fixed frequency $\nu_{\text{rf}}=56.3\text{ MHz}$. Fourier-transform echo recombination was used to record each spectrum, with a delay between pulses of $8 \mu\text{s}$ and a repetition time of 10 ms. The NMR integrated intensities of the various samples were identical within 20%. This ensures that all the Co nuclei are detected in the reported spectra. Isotropic shifts were evaluated using the center of gravity of the spectra, taking for the ⁵⁹Co gyromagnetic ratio $\gamma/2\pi=10.053\text{ MHz/T}$.

Typical Co NMR spectra are shown in Fig. 1 at $T=5\text{ K}$. A broad line is observed, together in some cases with a narrow peak due to the presence of about 10% of spurious Co₃O₄.¹² This explains why one cannot rely on macroscopic susceptibility measurements in these misfits: the Co₃O₄ paramagnetic contribution is too large to be safely subtracted. On the

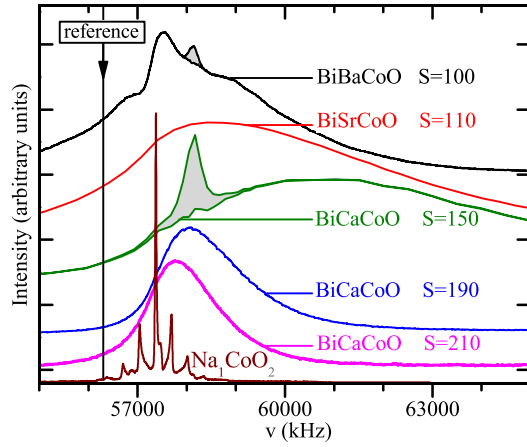


FIG. 1. (Color online) Co NMR spectra measured at $T=5$ K for various misfit compositions together with the undoped Na_1CoO_2 (Ref. 11). Related TEP values measured at $T=300$ K in $\mu\text{V}/\text{K}$ are indicated. In some cases, an additional Co_3O_4 spurious contribution is observed (gray shaded area).

contrary, with a local probe such as NMR, it is straightforward to measure the intrinsic CoO_2 susceptibility using the shift of the main line. As compared to the spectrum of non-oriented powder of Na_1CoO_2 , the misfit spectra are broader, more shifted, and do not show any set of satellite lines. In Na_1CoO_2 , these quadrupolar satellites originate from the effect of the electric field gradient (EFG) at the Co site.¹¹ In misfits, the incommensurability of the nearby RS layers strongly distributes the Co EFG, which could explain the absence of any quadrupolar structure. In addition, as we measure nonoriented powders, the large anisotropy of the hyperfine fields which occurs in doped CoO_2 layers¹³ leads to a distribution of the shift, i.e., an additional broadening. The sharp difference with Na_1CoO_2 where all Co are in +3 low-spin $S=0$ state implies that no isolated Co^{3+} ion is present in misfits on the time scale of NMR (~ 10 μs). We performed contrast measurements similar to those done in Na_xCoO_2 (Ref. 13) to probe the existence of different Co sites, by changing the delay between pulses in the NMR echo sequence. The whole line displays a homogeneous relaxation, implying that a unique Co valence state is detected, in contrast with the charge segregation observed in $\text{Na}_{0.67}\text{CoO}_2$. If any magnetic order were present, the spectra would split, broaden, or wipe out. This is not the case, which indicates the absence of spin order or freezing down to $T=5$ K in all compounds. We further checked this possibility by performing μSR measurements in the three BiCaCoO samples. As shown in Fig. 2, at $T=300$ K, a weak applied transverse field makes most of the polarization of the muons oscillate. This implies that no large internal field is present in the compound where muons were implanted. The weak Gaussian relaxation of the polarization (solid lines) reflects the existence of a small distribution of fields of a few gauss mainly due to the nuclear dipolar fields. On decreasing temperature, about 10–20% of the muon spins no longer oscillate because these muons belong to spurious phases such as CoO or Co_3O_4 , which order at $T_N=289$ and 34 K. In addition, the Gaussian envelope of the oscillating part narrows a little, implying the

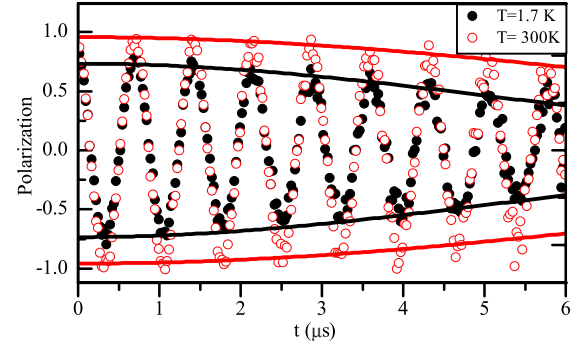


FIG. 2. (Color online) μSR polarization in a 100 G transverse field for BiCaCoO ($S=210$ $\mu\text{V}/\text{K}$) shows an oscillating behavior typical of a paramagnetic regime. The initial decrease with decreasing temperature originates from spurious contributions, while BiCaCoO remains nonmagnetic.

apparition of a small additional source of relaxation. If this were due to a spin ordering or freezing, we evaluated that it would correspond to moments of maximum $0.012\mu_B$ per cobalt atom in the worst and unlikely case where the muons would all stop as far as possible from Co layers. Measurements in zero field lead to similar conclusions. The two other BiCaCoO samples show similar behavior. In another μSR study, Sugiyama *et al.* also found no order down to $T=1.8$ and 2.3 K for BiBaCoO and BiSrCoO, respectively.⁶ But they argued that BiCaCoO showed spin freezing, in contrast to our findings. However, only 12% of their sample volume actually ordered, which is not significant. They further claimed that a universal dome-shaped relation between T_N and S occurred in all cobaltates. Our study performed on a *single* family and on a large range of S values rules out the universality of such a dome phase diagram for T_N . This unambiguously demonstrates that magnetic ordering is not responsible for or linked to the existence of a large TEP in cobaltates.

This absence of order sharply contrasts with the case of Na cobaltates, which become antiferromagnets at $T_N=19$, 22, and 28 K,¹⁴ as shown in Fig. 4(c) below. Incommensurability of misfits should play no role since BiBaCoO is commensurate. Therefore, either the much smaller interlayer distance in Na_xCoO_2 (~ 5 Å) than in misfits (~ 15 Å) or the Na crystallographic order may explain the antiferromagnetism. In the latter case, such order could be induced by a Co spatial charge ordering or by a reconstruction of the Fermi surface.

We now focus on the paramagnetic regime. The isotropic part of the shift of the NMR line, K_{iso} , is proportional to the magnetic susceptibility of Co. This shift is the only reliable way to determine the intrinsic susceptibility here, as already stressed above. As expected, K_{iso} is always higher and more T dependent than that of the band insulator Na_1CoO_2 , as shown in Fig. 3. In metallic BiBaCoO with low TEP, a flat behavior is observed, reminiscent of a metallic Pauli susceptibility. We measured a similar behavior in another low-TEP metallic TlSrCoO misfit whose structure and macroscopic properties are reported in Ref. 15. In contrast, in BiSrCoO and BiCaCoO, which are less metallic and have a higher S , the shift, and hence the susceptibility, follows a Curie-Weiss behavior (solid lines in Fig. 2):

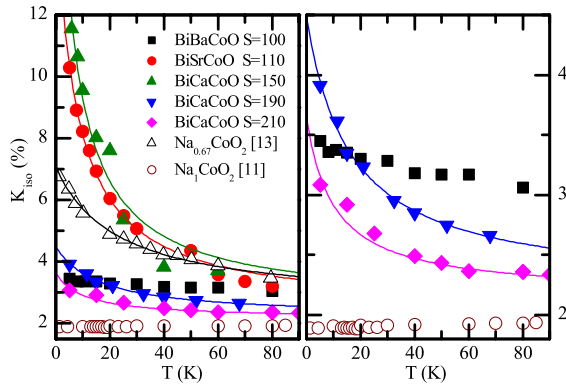


FIG. 3. (Color online) ^{59}Co NMR isotropic shift K_{iso} of the misfit compounds shown on two different scales (left and right panels). At low S , K_{iso} is flat, while it shows a Curie-Weiss behavior at higher S (full lines are Curie-Weiss fits).

$$K_{\text{iso}} = \frac{A_{\text{hf}}C}{T + \Theta} + K_{\text{orb}}^{\text{iso}}$$

where A_{hf} is the hyperfine coupling and $K_{\text{orb}}^{\text{iso}}$ is the T -independent orbital shift reported in Fig. 4(a). The Curie constant C first increases sharply with increasing S , and then decreases again. The Weiss temperature Θ is always lower than 100 K, but is hard to determine exactly from data taken on powders.

For a quantitative comparison with Na_xCoO_2 , we first need to evaluate the misfit Co layer doping. In Na_xCoO_2 , the Seebeck coefficient S at $T=300$ K scales almost linearly with x for $0.5 \leq x \leq 0.98$ as seen in Fig. 4(e).¹⁶ We use this arbitrary scaling to deduce an effective x doping in our misfit samples where we measured the TEP as well.¹⁷ From our measurement of S at $T=300$ K, we find $x=0.66(5)$, $0.69(5)$, $0.71(5)$, $0.79(3)$, $0.86(3)$, and $0.89(3)$ for TlSrCoO, BiBaCoO, BiSrCoO, and the three different BiCaCoO samples. This increase of x on decreasing the ion size ($\text{Ba} \rightarrow \text{Sr} \rightarrow \text{Ca}$) and hence decreasing the misfit parameter m ($2 \rightarrow 1.82 \rightarrow 1.67$) is consistent with electroneutrality. It is also the same as the one determined using the Fermi surface area for BiBaCoO.¹⁸ It is then possible to plot the various properties of misfit and Na cobaltates on a single x scale in Fig. 4, where we also included results we obtained on TlSrCoO. All families fall on a *unique* line for $K_{\text{orb}}^{\text{iso}}$ [Fig. 4(a)]. This strongly supports our phenomenological evaluation of x for misfits. The linear dependence of $K_{\text{orb}}^{\text{iso}}$ with Co valence could be linked to the crystal field splitting of the $t_{2g}-e_g$ level and its filling, as advocated in Ref. 13. The T dependence of the shift is evaluated in Fig. 4(b) using $\Delta K = K_{\text{iso}}(T=5 \text{ K}) - K_{\text{iso}}(T=80 \text{ K})$, a quantity that evolves like the Curie constant C , and which can be estimated for flat behavior as well. Misfit and Na cobaltates both evolve from a flat susceptibility to a Curie-Weiss dependence with increasing x . The very similar susceptibilities observed for both Bi and Na families at $x \approx 0.7$ in Figs. 3 and 4 imply that neither the interlayer distance nor the ordering of Na layers has a strong influence on the magnetic susceptibility at this doping. For $x \geq 0.75$, no reliable Na_xCoO_2 susceptibility data are available. The sus-

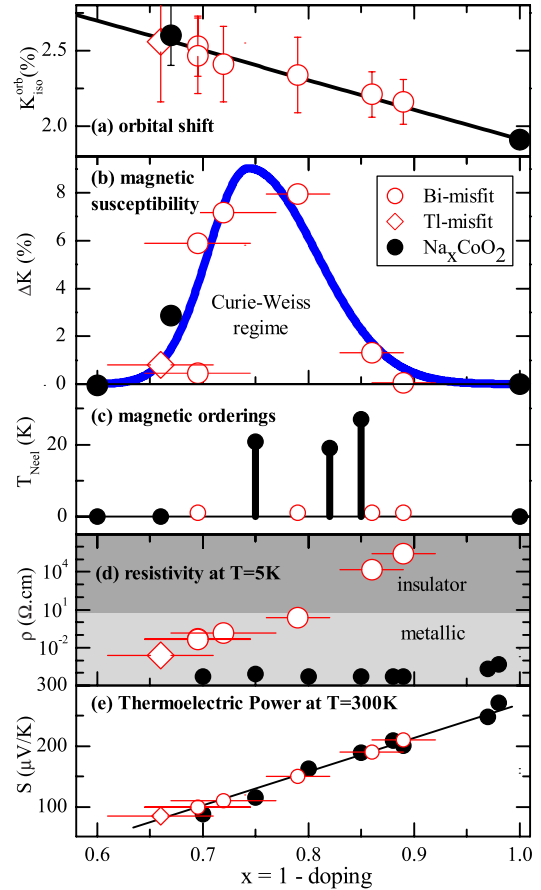


FIG. 4. (Color online) Phase diagram of misfit and Na cobaltates. (a) Isotropic orbital shift measured at $T=300$ K. (b) The T dependence of the misfit magnetic susceptibility evaluated through $\Delta K = K_{\text{iso}}(5 \text{ K}) - K_{\text{iso}}(80 \text{ K})$ and compared to published results for Na_xCoO_2 (Refs. 11–13). Blue line is a guide to the eye. (c) T_N in Na_xCoO_2 (Ref. 14) compared to the upper bound found for any order for misfit from this study and Ref. 6. (d), (e) ρ at $T=5$ K and S at $T=300$ K compared to Na_xCoO_2 single-crystal data of Ref. 16.

ceptibility still displays a Curie-Weiss behavior, but C decreases with increasing x . The Curie-Weiss temperature Θ also decreases from 50–100 K to 0–20 K within our limited accuracy. In a localized picture, higher x means a reduction of the number of spins and C , and an increase of the distance between spins, i.e., a decrease of Θ , as demonstrated in a t - J model.⁴ It is not obvious that Na_xCoO_2 would show similar dependences, since the Na Coulomb potential has been argued to induce strong correlations even at low doping.⁵

We finally report in Figs. 4(d) and 4(e) resistivity and TEP. The misfits evolve from an insulator to a metallic behavior on increasing doping, i.e., decreasing x , as will be detailed in Ref. 10. It is not surprising to find a metal-insulator transition when varying the hole doping ($1-x$). But one cannot understand along the same lines why Na cobaltates are good metals at all dopings. Recent angle-resolved photoemission spectroscopy measurements reveal as well qualitative differences in the dispersion curves for $x \geq 0.7$ between cobaltates and misfits.¹⁸ Perhaps specific arrangements of the Na allow for better hopping, or the RS incommensurability in misfits is detrimental to transport through

random potential scattering of the conduction electrons.

We address now the question of the TEP origin. While magnetic order, charge order, and good conductivity appear specific to Na_xCoO_2 , Curie-Weiss susceptibilities and large TEP are found in both Bi misfit and Na cobaltates and remain down to low dopings. We conclude that TEP is likely linked to the strong correlations within the Co layers, as proposed in Refs. 3, 4, and 19, rather than the band properties in a more conventional metallic picture.⁷ Understanding the nature of this link and how correlations result in the

properties summarized in Fig. 4 is an open and challenging issue. It is not only appealing on the fundamental side but also essential for thermoelectric applications using these strongly correlated materials in the future.

We acknowledge H. Alloul, I. Mukhamedshin, V. Brouet, and P. Limelette for fruitful discussions and A. Amato for assistance at the μSR facility. This work was supported by the ANR “OxyFonda” and by the EC FP 6 program, Contract No. RII3-CT-2003-505925.

-
- ¹G. D. Mahan, *Solid State Phys.* **51**, 81 (1998).
²I. Terasaki, Y. Sasago, and K. Uchinokura, *Phys. Rev. B* **56**, R12685 (1997); Y. Wang, N. S. Rogado, R. J. Cava, and N. P. Ong, *Nature (London)* **423**, 425 (2003).
³P. M. Chaikin and G. Beni, *Phys. Rev. B* **13**, 647 (1976); W. Koshibae, K. Tsutsui, and S. Maekawa, *ibid.* **62**, 6869 (2000).
⁴J. O. Haerter, M. R. Peterson, and B. S. Shastry, *Phys. Rev. B* **74**, 245118 (2006).
⁵C. A. Marianetti and G. Kotliar, *Phys. Rev. Lett.* **98**, 176405 (2007).
⁶J. Sugiyama, J. H. Brewer, E. J. Ansaldo, H. Itahara, T. Tani, M. Mikami, Y. Mori, T. Sasaki, S. Hébert, and A. Maignan, *Phys. Rev. Lett.* **92**, 017602 (2004).
⁷D. J. Singh, *Phys. Rev. B* **61**, 13397 (2000); Tsunehiro Takeuchi *et al. ibid.* **69**, 125410 (2004).
⁸M. Hervieu, Ph. Boullay, C. Michel, A. Maignan, and B. Raveau, *J. Solid State Chem.* **142**, 305 (1999); A. Maignan, S. Hébert, M. Hervieu, C. Michel, D. Pelloquin, and D. Khomskii, *J. Phys.: Condens. Matter* **15**, 2711 (2003); M. Hervieu, A. Maignan, C. Michel, V. Hardy, N. Créon, and B. Raveau, *Phys. Rev. B* **67**, 045112 (2003).
⁹T. Yamamoto, K. Uchinokura, and I. Tsukada, *Phys. Rev. B* **65**, 184434 (2002).
¹⁰S. Hébert, J. Bobroff, D. Pelloquin, and A. Maignan (unpublished).
¹¹G. Lang, J. Bobroff, H. Alloul, P. Mendels, N. Blanchard, and G. Collin, *Phys. Rev. B* **72**, 094404 (2005).
¹²We checked that the T -dependent shifts, widths, and transverse relaxation rates T_2 of this peak are those measured in pure Co_3O_4 by T. Fukai, Y. Furukawa, S. Wada, and K. Miyatani, *J. Phys. Soc. Jpn.* **65**, 4067 (1996).
¹³I. R. Mukhamedshin, H. Alloul, G. Collin, and N. Blanchard, *Phys. Rev. Lett.* **93**, 167601 (2004); **94**, 247602 (2005).
¹⁴S. P. Bayrakci, C. Bernhard, D. P. Chen, B. Keimer, R. K. Kremer, P. Lemmens, C. T. Lin, C. Niedermayer, and J. Strempler, *Phys. Rev. B* **69**, 100410(R) (2004); P. Mendels, D. Bono, J. Bobroff, G. Collin, D. Colson, N. Blanchard, H. Alloul, I. Mukhamedshin, F. Bert, A. Amato, and A. D. Hillier, *Phys. Rev. Lett.* **94**, 136403 (2005).
¹⁵S. Hébert, S. Lambert, D. Pelloquin, and A. Maignan, *Phys. Rev. B* **64**, 172101 (2001).
¹⁶Minhyea Lee, Liliana Viciu, Lu Li, Yayu Wang, M. L. Foo, S. Watauchi, R. A. Pascal, Jr., and R. J. Cava, and N. P. Ong, *Nat. Mater.* **5**, 537 (2006).
¹⁷All the T dependences of the TEP show the same behavior as the one reported in Refs. 8 and 15.
¹⁸V. Brouet, A. Nicolaou, M. Zacchigna, A. Tejada, L. Patthey, S. Hébert, W. Kobayashi, H. Muguerra, and D. Grebille, *Phys. Rev. B* **76**, 100403 (2007).
¹⁹P. Limelette, S. Hébert, V. Hardy, R. Frésard, Ch. Simon, and A. Maignan, *Phys. Rev. Lett.* **97**, 046601 (2006).